

The evolution of elastic moduli with increasing crack damage during cyclic stressing of a basalt from Mt. Etna volcano

M.J. Heap^{a,*}, S. Vinciguerra^b, P.G. Meredith^a

^a Rock & Ice Physics Laboratory, Department of Earth Sciences, University College London, Gower Street, London WC1E 6BT, UK

^b Istituto Nazionale di Geofisica e Vulcanologia, sezione di Roma1 - Via di Vigna Murata 605, 00143, Rome, Italy

ARTICLE INFO

Article history:

Received 21 January 2008
Received in revised form 29 September 2008
Accepted 3 October 2008
Available online 10 October 2008

Keywords:

Cyclic stressing
Etna basalt
Elastic moduli
Crack damage
Acoustic emissions

ABSTRACT

Volcanic edifices, such as Mt. Etna (Italy), are commonly subject to repeated cycles of stress over time due to the combination of magma emplacement from deep reservoirs to shallow depths and superimposed tectonic stresses. Such repeated stress cycles lead to anisotropic deformation and an increase in the level of crack damage within the rocks of the edifice and hence changes to their elastic moduli, which are a key parameter for reliable modelling of deformation sources. We therefore report results of changes in elastic moduli measured during increasing amplitude cyclic stressing experiments on dry and water-saturated samples of Etna basalt. In all experiments, the Young's modulus decreased by approximately 30% over the total sequence of loading cycles, and the Poisson's ratio increased by a factor of approximately 3 ± 0.5 . Microseismicity, in terms of acoustic emission (AE) output, was also recorded throughout each experiment. Our results demonstrate that AE output only re-commences during any loading cycle when the level of stress where AE ceased during the unloading portion of the previous cycle is exceeded; a manifestation of the Kaiser stress-memory effect. In cycles where no AE output was generated, we also observed no change in elastic moduli. This result holds for both mechanical and thermal stressing. Our results are interpreted in relation to measurements of volcano-tectonic seismicity and deformation at Mt. Etna volcano.

© 2008 Elsevier B.V. All rights reserved.

1. Introduction

Elastic moduli are the key parameters for defining relationships between stress and strain. They determine the distribution and magnitude of sub-yield stresses, the propagation velocity of elastic (seismic) waves and can be used to relate strain measurements to in-situ stresses within the Earth's crust. In volcanic regions, reliable estimates of mechanical properties and their degradation under multiple episodes of stressing are crucial to the accurate modelling of routinely monitored data such as ground deformation, and the calibration of damage-mechanics criteria for the weakening of rocks forming volcanic edifices.

Mt. Etna is Europe's largest volcano, and one of the most active on Earth. It lies near the eastern (Ionian) coast of Sicily (Italy) (Fig. 1). Mt. Etna is a stratovolcano formed by the superposition of several volcanic edifices, has a volume of at least 350 km³ and a height of about 3300 m. It is one of the most densely monitored volcanoes on the planet and has a documented record of eruptions extending to several centuries BC. The geological and structural complexity of Mt. Etna means that the mechanisms by which magma rises to the surface and drives volcanic eruptions are still not fully understood. However,

volcanic activity on Mt. Etna may be divided into two main types: (1) persistent activity with episodic paroxysmal events, which generally occurs at or near the summit and is not preceded by seismic precursors (e.g. Lombardo and Cardaci, 1994), and (2) cycles of hazardous flank eruptions (Guest, 1982), which are preceded by intense seismic activity (Castellano et al., 1997; Vinciguerra et al., 2001), often including shallow destructive earthquakes (Azzaro et al., 2000), which indicates the acceleration of brittle failure mechanisms (Patanè et al., 2004). Over the last 20 years, new technological developments and denser monitoring networks at Mt. Etna volcano have provided one of the highest quality volcanological, geophysical and geochemical data sets for any volcano in the world (Bonaccorso et al., 2004a). Following the 1991–1993 eruption, the largest effusive eruption of the 20th century (Patanè et al., 1996), the volcano has experienced a cycle of intense activity (Allard et al., 2006 and references therein) evolving from (1) initial recharging of the plumbing system and inflation, to (2) powerful summit eruptions and, finally, to (3) a sequence of flank eruptions accompanied by major slip of the eastern flank and intense fracturing. In this framework, pre-eruptive patterns defined from seismic fault plane solutions and deformation events (Bonaccorso et al., 1996; Patanè et al., 2003, 2006) suggest that magma intrusion has induced strike-slip faulting within a strongly anisotropic stress field. Importantly, a number of field and monitoring based studies have revealed that open fissures were formed first, and magma was then extruded through

* Corresponding author.

E-mail address: m.heap@ucl.ac.uk (M.J. Heap).

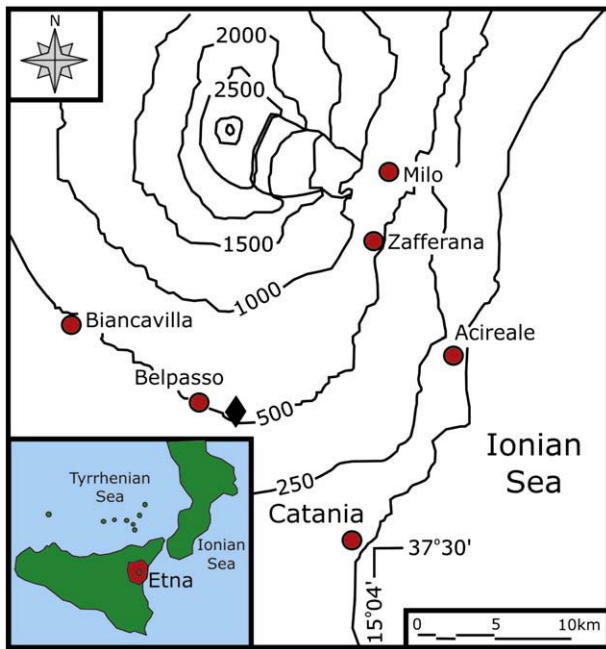


Fig. 1. Location map of Mt. Etna showing main towns and morphological features. The solid diamond indicates the position of the quarry from which the EB test material was collected.

these fissures at a later stage (Tibaldi and Groppelli, 2002; Branca et al., 2003; Alparone et al., 2004; Carbone and Greco, 2007).

Taken together, these observations suggest that repeated episodes of deformation can lead, through brittle mechanisms, to an increase in the level of crack damage within the rocks of the edifice, and hence to changes in their elastic moduli. Furthermore, quantifying the mechanical properties, such as the elastic moduli and strength, of the rocks constituting Mt. Etna volcano's edifice is of key importance in establishing the reliability of modelled deformation sources. This is because values for the elastic moduli (in particular Young's modulus and Poisson's ratio) are essential input parameters for such models. Previous studies of Mt. Etna volcano have assumed fixed values of Young's modulus ranging from 50 to 100 GPa and a Poisson's ratio of 0.25 (Cayol and Cornet, 1998; Bonaccorso and Davis, 1999).

Basaltic rocks from Mt. Etna volcano have been the subject of a number of mechanical studies in recent years. In an attempt to characterize fracture propagation, Ciccotti et al. (2000) measured mode I subcritical crack growth parameters. Also, quantitative investigations of lava flow fracturing dynamics have been pursued through mechanical tests in both tension (Balme et al., 2004) and compression (Rocchi et al., 2004) at high temperatures and low pressures. Under compression, their extrusive basalt exhibited a low strength of around 100 MPa that varied little with confining pressure, and a low Young's modulus around 40 GPa at temperatures up to 600 °C. Above this temperature both strength and elastic modulus were observed to decrease even further (Rocchi et al., 2004). Investigations of the physical properties of the basalt used in this study have yielded unexpectedly low ultrasonic wave velocities and unexpectedly high fluid permeability. Both observations have been attributed to the presence of a high level of connected pre-existing microcrack damage (Vinciguerra et al., 2005). Such microcracks are interpreted as being of thermal origin, since values of physical properties are not affected by further thermal stressing (Vinciguerra et al., 2005).

Numerous experimental studies have also shown that, generally for crystalline rocks, the level of microcrack damage greatly influences both static (Alm et al., 1985; Martin and Chandler, 1994; Eberhardt et al., 1999;

Lau and Chandler, 2004; Heap and Faulkner, 2008) and dynamic (Birch, 1960, 1961; Walsh, 1965; Anderson et al., 1974; O'Connell and Budiansky, 1974; Soga et al., 1978; Ayling et al., 1995; Sayers and Kachanov, 1995; Guéguen and Schubnel, 2003; Reuschlé et al., 2003; Fortin et al., 2005; Takemura and Oda, 2005) elastic moduli. Therefore, each stress cycle within a volcanic edifice can result in an increase in the level of crack damage, as evidenced by the output of seismic energy.

Here, we report results from an experimental study in which we measured the degradation of elastic moduli during cyclic stressing of samples of an extrusive basalt from Mt. Etna volcano to increasing levels of maximum stress. Acoustic emission (AE) output was recorded continuously during each cycle of each experiment as a proxy for the onset of increasing crack damage.

2. Material investigated and experimental methodology

The most representative basalt from Mt. Etna volcano is a porphyritic, intermediate, alkali basalt (Tanguy et al., 1997). The Etna basalt used in this study (collected from the location indicated in Fig. 1, and hereinafter called EB) has a bulk density of 2700 kg m^{-3} , a connected porosity (measured with a helium pycnometer) of 4.4% and a total porosity of 4.8%. It is composed of a fine-grained groundmass (~60%), with crystals of feldspar (25%), pyroxene (8.5%) and olivine (4%). In its as-received state, EB has an anomalously low ultrasonic *P*-wave velocity for basalt of approximately 3.2 km s^{-1} , which exhibits essentially zero anisotropy under ambient laboratory conditions. These characteristics have been attributed to an extensive pre-existing network of interconnected microcracks of thermal origin, caused by the relatively fast cooling rates of Mt. Etna lava flows (Vinciguerra et al., 2005).

In this study, increasing-amplitude, stress-cycling experiments were performed on both oven-dry (at 80 °C, see Glover et al., 1995) (hereinafter referred to as 'dry') and water-saturated (hereinafter referred to as 'wet') samples of EB to investigate the evolution of crack damage and elastic moduli during cyclic loading. All samples were cored from the same block of material to a diameter of 25 mm and were precision-ground to 75 mm in length, resulting in a length:diameter ratio of 3:1 (Mogi, 1966; Hawkes and Mellor, 1970). All experiments were performed in a servo-controlled, uniaxial loading frame and were conducted at room temperature. Axial and radial strains were continuously monitored throughout each experiment using displacement transducers. Output of AE energy, used as a proxy measure for the onset of new crack damage, was recorded by a MISTRAS-2001 AE recording system via a broadband PZT piezoelectric AE transducer located inside the bottom loading anvil (Fig. 2). The AE transducer has a high response band over the range from 100 kHz–1 MHz and data was recorded at a sampling rate of 10 MHz. Cumulative AE energy was calculated by summing the envelope of each AE waveform (see Cox and Meredith, 1993 for a detailed description of the AE recording methodology). The experimental arrangement is shown in Fig. 2. A series of constant strain rate ($7.0 \times 10^{-6} \text{ s}^{-1}$) experiments were performed on dry samples of EB prior to the stress-cycling experiments in order to determine the unconfined compressive strength (UCS). This is required to guide the choice of the amplitude and frequency of cycles during stress-cycling experiments.

During the increasing-amplitude stress-cycling experiments, samples were first loaded to a maximum stress of 20 MPa at a controlled strain rate of $7.0 \times 10^{-6} \text{ s}^{-1}$, and then unloaded at the same rate to 8 MPa. In each subsequent cycle the maximum stress was increased by 10 MPa, and samples again unloaded to 8 MPa. Stress-cycling was continued in this way until samples eventually failed. Fig. 3 shows an example of a loading path for a dry sample that failed on the 14th loading cycle.

3. Results

Fig. 4 shows the stress-strain curves from one of a series of constant strain rate experiments on EB that yielded a mean UCS of $140 \pm 5 \text{ MPa}$.

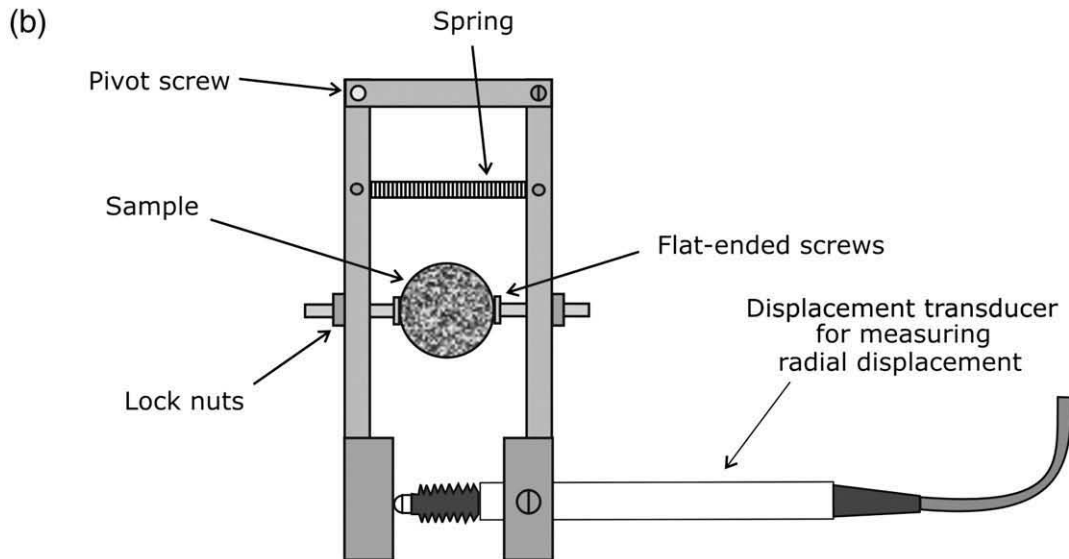
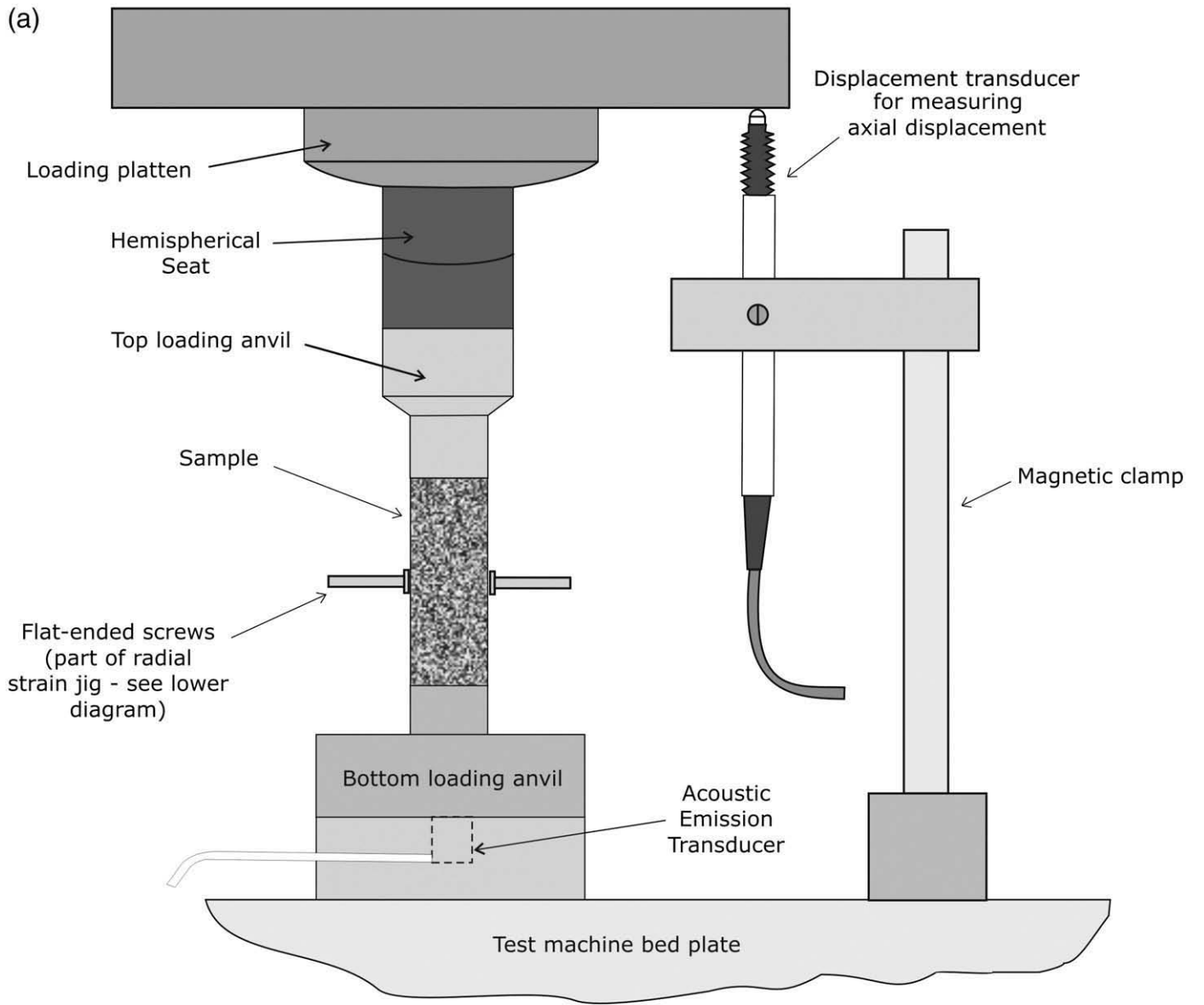


Fig. 2. Schematic diagram of the experimental arrangement: (a) elevation showing the loading components and the positions of the axial displacement and AE transducers; (b) plan view showing the arrangement for measurement of radial displacement.

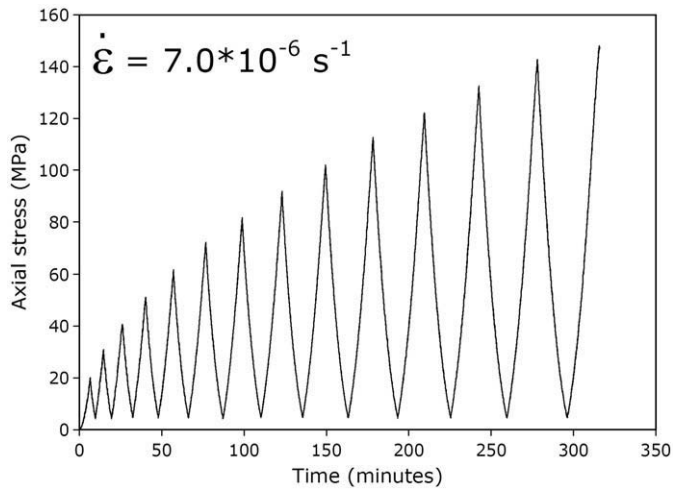


Fig. 3. Example of a loading path from an increasing-amplitude, cyclic stressing experiment on an oven-dry sample of EB that failed during the 14th loading cycle. Strain rate is indicated on the figure.

Fig. 5 shows representative stress–strain curves from cyclic loading experiments on both dry (Fig. 5a) and wet (Fig. 5b) samples of EB. It is apparent that the stress–strain response of the rock varies between loading cycles, and this is most easily seen in the radial strain curves. Eventually the samples failed, generally by axial splitting as illustrated in Fig. 6.

Each of the loading portions of the stress–strain curves was fitted with a third-order polynomial and the static elastic moduli were calculated from the quasi-linear central portion of each curve using the method described by Heap and Faulkner (2008). Fig. 7 shows the calculated values of Young's modulus and Poisson's ratio plotted against cycle number. The elastic response to stress-cycling is similar for both dry and wet samples. In both cases, Young's modulus is seen to decrease by about 30%, with Poisson's ratio increasing by 0.29. This corresponds to a Poisson's ratio increase by a factor of between 2.5 and 3.0 for dry and wet samples respectively, due to their somewhat different starting values.

AE output from one of the experiments on a dry sample is shown in Fig. 8, plotted against stress and time. During most cycles, AE output is observed to commence just prior to the maximum stress on the previous cycle. In general, we find that AE output re-commences during any loading cycle at the same level of stress that it ceased

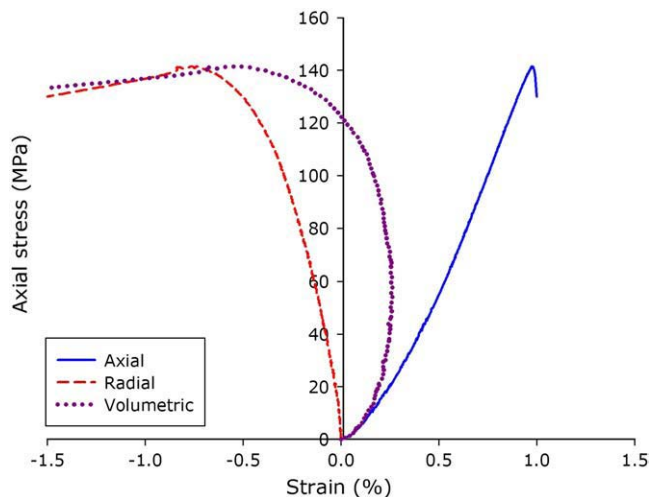


Fig. 4. Plot of uniaxial stress against axial, radial and volumetric strain for an oven-dry sample of EB deformed under a constant strain rate of $7.0 \times 10^{-6} s^{-1}$ until failure. This sample failed at approximately 140 MPa.

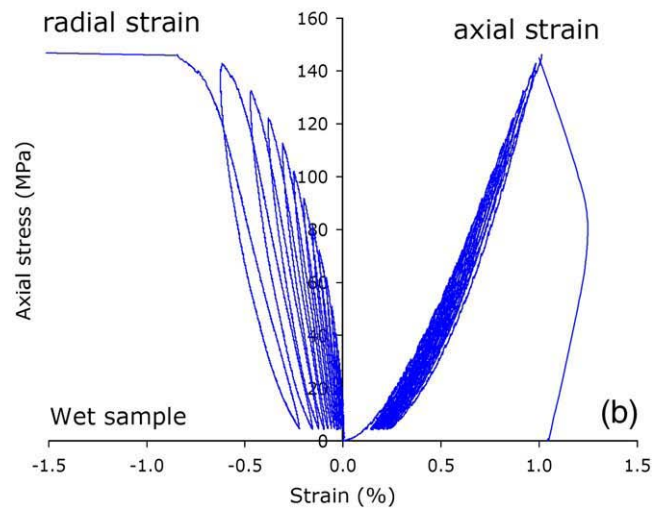
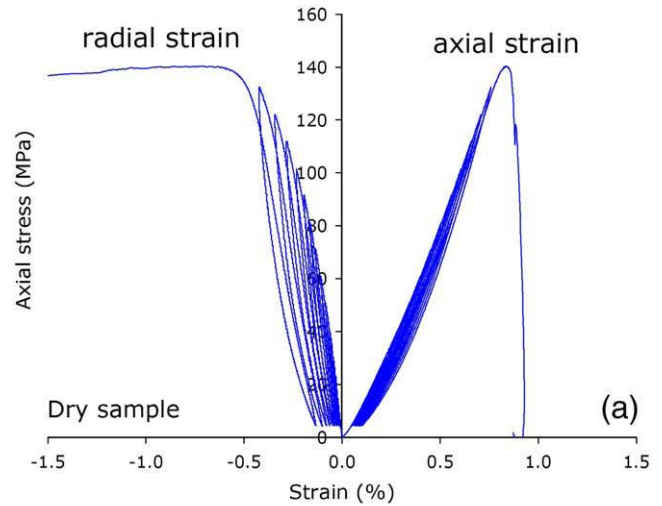


Fig. 5. Representative axial and radial stress–strain curves for: (a) oven-dry and (b) water-saturated EB samples during increasing-amplitude cyclic stressing experiments. The volumetric strain curves have been excluded to aid clarity.

during the unloading portion of the previous cycle. We also note that the amount of AE energy emitted during the final loading cycle, where microcracks link and coalesce to produce the type of macroscopic failure shown in Fig. 6, is much greater than for any of the preceding cycles.

4. Discussion

The progressive degradation of sample stiffness that results in the Young's modulus reduction and Poisson's ratio increase is primarily attributed to an increase in the level of crack damage within the samples; either the extension of favourably-oriented, pre-existing cracks, the propagation of new cracks, or some combination of both. Each cycle that loads the sample to a higher stress imparts an additional increment of crack damage to the sample, leading to increasing amounts of irrecoverable strain.

The evolution of both Young's modulus and Poisson's ratio with increasing damage level is qualitatively similar to the pattern reported by Heap and Faulkner (2008) from stress-cycling experiments on Westerly granite. However, they found that Young's modulus for their granite samples decreased by a total of about 11%, and Poisson's ratio increased by a factor of about 1.7 over the total duration of their uniaxial stress-cycling experiments; considerably less than we observe for our EB samples. We suggest that EB exhibits a greater

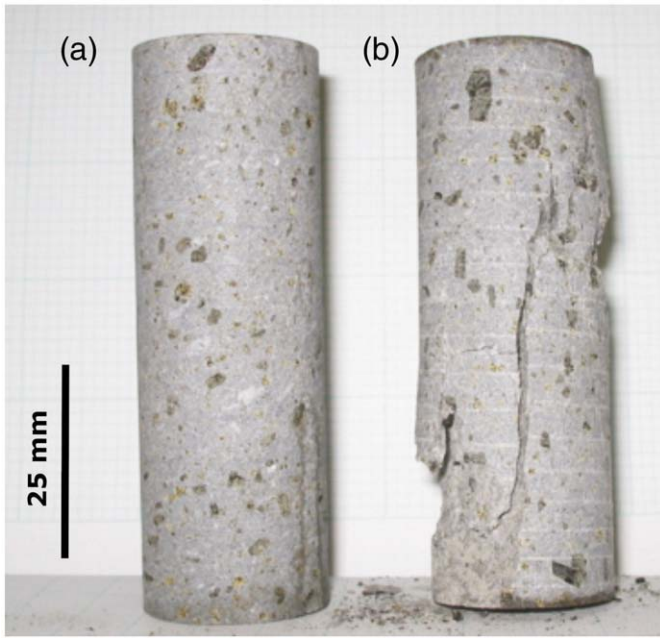


Fig. 6. Photographs of: (a) an undeformed sample of EB, and (b) a sample of EB that failed by axial splitting after 14 load cycles of an increasing-amplitude cyclic stressing experiment.

increase in Poisson's ratio than Westerly granite due to its low initial value; the result of a high degree of pre-existing microcrack damage present within the rock (Vinciguerra et al., 2005; Benson et al., 2006). In contrast, Westerly granite contains a very low initial crack density (Hadley, 1976). In general, a higher level of pre-existing crack damage (as in our EB samples) results in a lower initial Poisson's ratio. However, when we increase the level of crack damage through cyclic stressing, the Poisson's ratio also increases. This appears to be a contradiction, but it is not. The pre-existing crack damage in EB is known to be isotropically distributed (Vinciguerra et al., 2005; Benson et al., 2006). Therefore, radial cracks oriented sub-normal to the direction of the applied stress are easily closed when that stress is first applied. This leads to a relatively low radial strain and a low initial Poisson's ratio. By contrast, when the stress is high enough to generate new cracks, these are preferentially oriented parallel to the applied stress (i.e. axially). They therefore open easily when stress is re-applied on the next loading cycle, leading to a high radial strain and a high Poisson's ratio. The same conclusion was drawn by Heap and Faulkner (2008) in their study of cyclic loading of Westerly granite.

In our experiments we observe no significant difference in the evolution of elastic moduli with increasing damage between dry and wet samples of EB. Wet samples are considered to be more relevant to field observations (Vinciguerra et al., 2006) where rocks are expected to be saturated in the sub-surface. Furthermore, it is well-known that the values of elastic moduli are frequency dependent (e.g. Vinciguerra et al., 2006). Therefore, fluid saturation has a significant influence on dynamic elastic moduli measured at ultrasonic frequencies (Winkler and Murphy, 1995; Vinciguerra et al., 2006), due to rapid energy dissipative mechanisms such as 'fluid squirt'. However, in our experiments, where we have measured static elastic moduli at a frequency some nine orders of magnitude lower than ultrasonic frequencies, we would only expect water-saturation to affect the mechanical/elastic behaviour of the rock through the law of effective stress. However, that law has no effect on the results of our experiments because they were conducted at atmospheric pressure without a pressurized pore fluid.

Previous AE studies of cracking in rocks have demonstrated that, in general, new microcrack damage is generated only once the previous maximum stress has been exceeded during cyclic loading. This

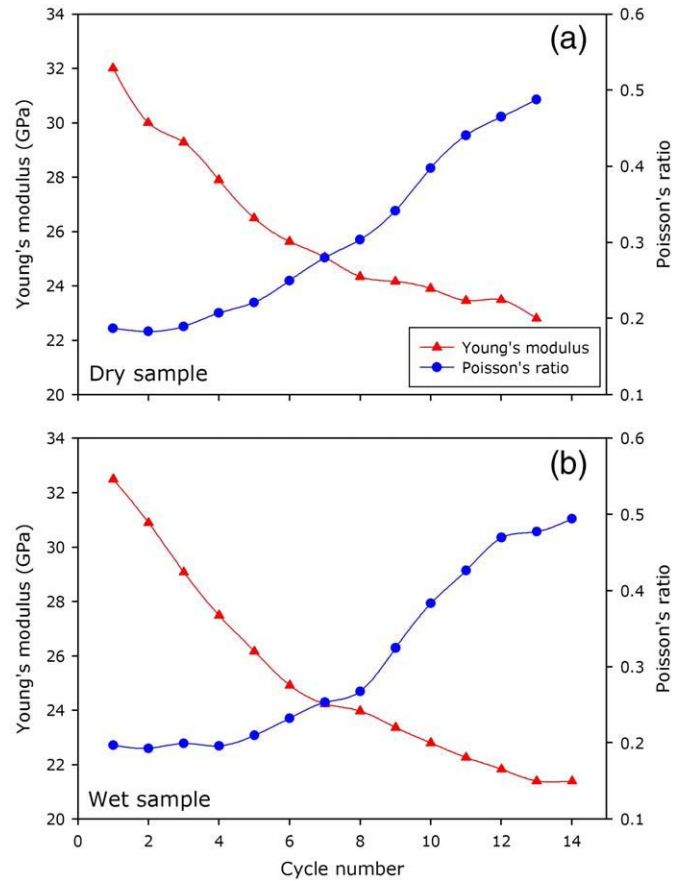


Fig. 7. Evolution of static elastic moduli for: (a) a dry sample of EB and (b) a wet sample of EB, as a function of cycle number, during increasing-amplitude, cyclic stressing experiments.

phenomenon was first reported in metals (Kaiser, 1953) and is now known as the Kaiser 'stress-memory' effect (see reviews by Holcomb, 1993; Lockner, 1993; Lavrov, 2003). However, Fig. 8 shows that, in our experiments, AE output re-commenced during any loading cycle at the same level of stress that it ceased during the unloading portion of the previous cycle. We do not therefore see a classical manifestation of the Kaiser stress-memory effect. Since the samples were not held at the maximum stress on any cycle for any extended period of time, crack damage did not have time to equilibrate to the level of applied

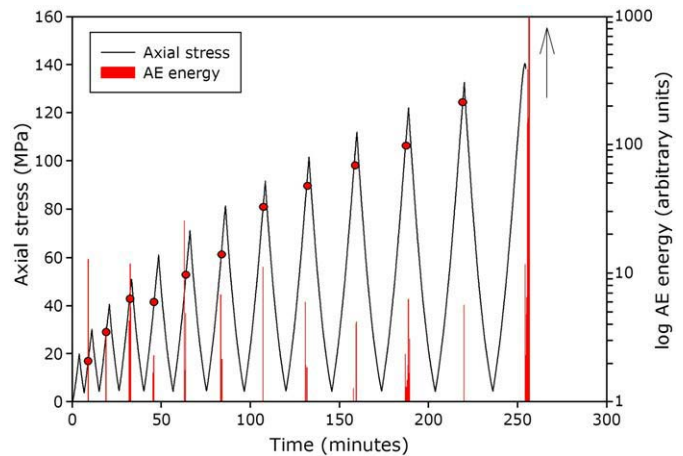


Fig. 8. Output of acoustic emission (AE) energy, as a function of stress and time, from an increasing-amplitude, cyclic stressing experiments on a dry sample of EB. Solid circles indicate the points at which AE activity recommenced on each loading cycle.

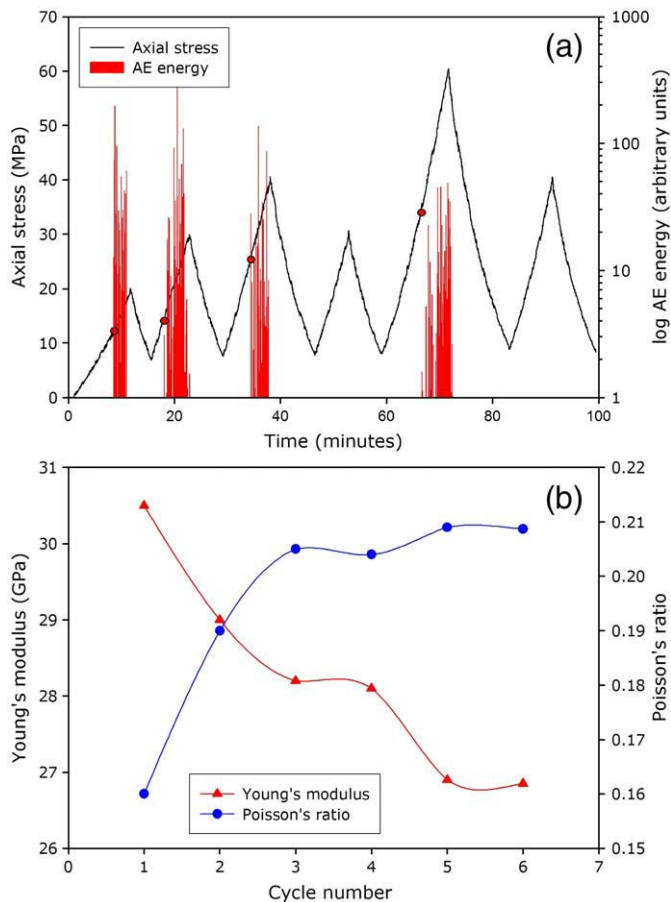


Fig. 9. Results from a cyclic stressing experiment on a dry sample of EB in which the maximum stress in each cycle has been randomly selected to be either higher or lower than that of the previous cycle: (a) output of AE energy, and (b) evolution of elastic moduli.

stress. Consequently, time-dependent subcritical cracking continues during a small portion of the unloading part of that cycle.

However, during the complex pattern of stressing that can act over extended time within volcanic edifices, the stress acting on the rock during any loading/pressurization cycle may not necessarily exceed that during the previous cycle. Under these circumstances, the Kaiser effect would predict that no further crack damage would be generated in those cycles where the stress did not exceed the previous maximum. We have therefore performed stress-cycling experiments in which the maximum stress in each cycle has been randomly selected to be either higher or lower than that of the previous cycle, in order to gain a better understanding of this more realistic scenario. In this case we observed a more complex manifestation of the Kaiser effect, as expected, where significant AE output in any cycle was only observed when the stress in that cycle exceeded the maximum stress on any previous cycle (as shown in Fig. 9a). The evolution of the elastic moduli for this experiment, calculated exactly as previously described, is shown in Fig. 9b. It is clear that changes in the elastic moduli are only observed during cycles that are accompanied by AE output, and in which the maximum stress exceeded that on any previous cycle. We therefore suggest that, in nature, only those stress episodes that are accompanied by volcano-seismicity will result in extra damage to the edifice and lead to changes in elastic moduli and seismic velocities. A number of specific mechanisms have been proposed for the origin of volcano-tectonic earthquakes (e.g. Hill, 1977; Ukawa and Tsukahara, 1996; Roman and Cushman, 2006). However, our interpretation is consistent with all of these, and also with detailed seismological studies at Mt. Etna volcano over many years which demonstrate that

volcano-tectonic events occur before and during flank eruptions, involving fracturing and dyke propagation (Bonaccorso et al., 1996, 2004b), but that no volcano-tectonic events are observed before and during summit eruptions, which occur along open conduits (Lombardo and Cardaci, 1994).

The brittle response of the volcanic edifice to the stress induced by dyke propagation also needs to take account of any elevated temperature and/or temperature fluctuation linked to magma intrusion. However, previous work on EB (Vinciguerra et al., 2005) concluded that thermal stressing did not lead to the creation of further crack damage if the temperature did not exceed that already experienced by the rock during the process of cooling from a lava flow. For example, Vinciguerra et al. (2005) reported no significant change from ambient temperature values of *P*-wave velocity, *S*-wave velocity or fluid permeability in samples of EB that were thermally stressed to 300°, 600° and 900 °C. This is, in essence, a manifestation of the thermal equivalent of the Kaiser effect seen in mechanical stressing.

Nevertheless, we have performed stress cycling experiments on the thermally-stressed samples of EB in order to ascertain if the above observation for physical and transport properties also holds for mechanical and elastic properties. Samples were heated in a tube furnace at a constant rate of 1 °C/min to 900 °C, held at that temperature for one hour to equilibrate, and then cooled to ambient temperature at the same rate. Results from a cyclic-stressing experiment on a heat-treated sample are shown in Fig. 10, and should be compared with the data of Fig. 7. Overall, the results are very similar; both in the absolute values of the Young's modulus and Poisson's ratio and in their changes during stress cycling. For example, over 13 stress cycles the Young's modulus of the heat-treated sample decreased by 30%; the same change observed for the untreated samples (Fig. 7). During the same experiment, the Poisson's ratio of the heat-treated sample increased by 0.33; a little more than the increase of 0.29 observed for the non-heat-treated samples, and likely due to the slightly lower starting value of Poisson's ratio for the heat-treated sample.

Overall, our observations of changes in elastic moduli during cyclic-stressing of heat-treated EB samples are in agreement with the observations of changes in physical and transport properties reported by Vinciguerra et al. (2005). That is, that thermal stressing up to 900 °C does not induce any new crack damage into samples of EB, and hence does not induce any significant change in the response to mechanical loading. This is consistent with the observation that during the final stages of dyke intrusion (higher temperatures and lower pressures), only low magnitude earthquakes occur, while during the early stages of intrusion (lower temperatures and higher pressures) activation of

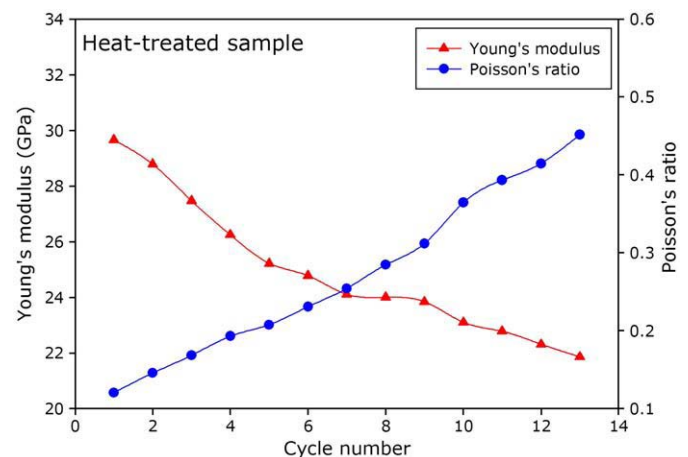


Fig. 10. Evolution of static elastic moduli during an increasing-amplitude, cyclic stressing experiment on a sample of EB that had previously been thermally stressed to 900 °C.

focal volumes and brittle deformation of the volcanic pile is observed, indicated by higher magnitude volcano-tectonic events (Patanè et al., 2004 and references therein). It should be noted, however, that during extended periods of volcano quiescence, elevated temperatures could lead to time-dependent healing of some of the microcrack damage caused by the cyclic stressing, and thus at least partially re-set the clock (see e.g., Hickman and Evans, 1987).

The changes in static elastic moduli observed during our experiments are large. However, large changes in elastic wave velocities are also observed in volcanic rocks upon the introduction of new crack damage (Vinciguerra et al., 2005; Stanchits et al., 2006). For example, Vinciguerra et al. (2005) report a 40% decrease in the *P*-wave velocity of initially undamaged Seljadur basalt after thermal stressing to 900 °C. The variation in static elastic moduli is currently unknown for volcanic edifices, since in-situ measurements are inevitably dynamic values derived from seismic wave velocities, and it has long been recognized that elastic moduli values are frequency dependent (Simmons and Brace, 1965; Cheng and Johnston, 1981; Eissa and Kazı, 1989; Ciccotti and Mulargia, 2004; Ciccotti et al., 2004) due to intrinsic anelasticity. We suggest that static moduli are more representative than dynamic moduli in modelling the deformation of volcanic edifices, because the pre-eruptive deformation of such edifices proceeds quasi-statically rather than dynamically (e.g. Kilburn, 2003). Furthermore, our static moduli measurements are made on laboratory samples that are extensively damaged during our experiments. Hence our measurements are characteristic of the whole sample. By contrast, dynamic measurements calculated from elastic wave velocities through volcanic edifices are average values for the whole edifice. Since only a small proportion of the total volume of the edifice is likely to be damaged by new crack growth during any pressurization cycle, we would only expect commensurately smaller changes in the average dynamic moduli. We also note that our results exhibit very similar trends to those previously published by Heap and Faulkner (2008) and Eberhardt et al. (1999) who used similar techniques.

5. Conclusions

- (1) We have demonstrated that cyclic stressing significantly changes the static elastic moduli of EB. In all cases where the maximum stress was increased in successive cycles, the Young's modulus is seen to decrease by about 30% and the Poisson's ratio to increase by a factor of 3 ± 0.5 . These changes are attributed to an increase in the level of crack damage with increasing stress in each cycle.
- (2) AE (micro-seismicity) output is seen to re-commence during any loading cycle at the same level of stress at which it ceased during the unloading portion of the previous cycle. Where the stress in any loading cycle does not reach that at which AE ceased in the preceding cycle, then no further AE output is observed and the elastic moduli do not change. We therefore conclude that no further crack damage is created during these cycles. We further suggest that, in nature, only those stress episodes that are accompanied by volcano-seismicity will result in extra damage to the edifice and lead to changes in elastic moduli and seismic velocities. This suggestion is in agreement with the results of long-term seismological monitoring at Mt. Etna volcano (Lombardo and Cardaci, 1994; Bonaccorso et al., 1996, 2004a,b).
- (3) We also find that slow thermal stressing of EB samples to 900 °C does not result in any increase in crack damage or degradation of elastic moduli. These observations are entirely in agreement with the experimental observations of no changes in physical and transport properties of thermally stressed EB reported by Vinciguerra et al. (2005), and with the seismological data reported by Patanè et al. (2004).

Acknowledgements

We gratefully acknowledge John Bowles for the design and construction of the radial strain jig, Steve Boon for development and implementation of the digital control system and Neil Hughes for help and support during experimentation. The authors would also like to acknowledge P. Baud and A. Manconi for fruitful discussions and our reviewers for their helpful comments and suggestions that improved this manuscript. M. H. was funded by NERC studentship NER/S/A2005/13553 and S. V. was supported by project FIRB-MIUR (Sviluppo Nuove Tecnologie per la Protezione e Difesa del Territorio dai Rischi Naturali) and NEST Pathfinder Program Triggering Instabilities in Materials and Geosystems (contract NEST-2005-PATH-COM-043386).

References

- Allard, P., Behncke, B., D'Amico, S., Neri, M., Gambino, S., 2006. Mount Etna 1993–2005: anatomy of an evolving eruptive cycle. *Earth Sci. Rev.* 78, 1–2.
- Alm, O., Jaktlund, L., Shaoquan, K., 1985. The influence of microcrack density on the elastic and fracture mechanical properties of Stripa granite. *Phys. Earth Planet. Inter.* 40, 161–179.
- Alparone, S., Andronico, D., Giammanco, S., Lodato, L., 2004. A multidisciplinary approach to detect active pathways for magma migration and eruption at Mt. Etna (Sicily, Italy) before the 2001 and 2002–2003 eruptions. *J. Volcanol. Geotherm. Res.* 136, 121–140.
- Anderson, D.L., Minster, B., Cole, D., 1974. The effect of orientated cracks on seismic velocities. *J. Geophys. Res.* 79, 4011–4015.
- Ayling, M.R., Meredith, P.G., Murrell, S.A.F., 1995. Microcracking during triaxial deformation of porous rocks monitored by changes in rock physical properties. I. Elastic-wave propagation measurements on dry rocks. *Tectonophysics* 245, 205–221.
- Azzaro, R., Barbano, M.S., Antichi, B., Rigano, R., 2000. Macroseismic catalogue of Mt. Etna earthquakes from 1832 to 1998. *Acta Vulcanol.* 12 (1/2), 3–36.
- Balme, M.R., Rocchi, V., Jones, C., Sammonds, P.R., Meredith, P.G., Boon, S., 2004. Fracture toughness measurements on igneous rocks using a high-pressure, high-temperature rock fracture mechanics cell. *J. Volcanol. Geotherm. Res.* 132, 159–172.
- Benson, P., Schubnel, A., Vinciguerra, S., Trovato, C., Meredith, P.G., Young, R.P., 2006. Modeling the permeability evolution of microcracked rocks from elastic wave velocity inversion at elevated isostatic pressure. *J. Geophys. Res.* 111, B04202. doi:10.1029/2005JB003710.
- Birch, F., 1960. The velocity of compressional waves in rocks to 10 kilobars, 1. *J. Geophys. Res.* 65, 1083–1102.
- Birch, F., 1961. The velocity of compressional waves in rocks to 10 kilobars, 2. *J. Geophys. Res.* 66, 2199–2224.
- Bonaccorso, A., Davis, P.M., 1999. Models of ground deformation from vertical volcanic conduits with application to eruptions of Mount St. Helens and Mount Etna. *J. Geophys. Res.* 104, 10531–10542.
- Bonaccorso, A., Ferrucci, F., Patanè, D., Villari, L., 1996. Fast deformation processes and eruptive activity at Mount Etna (Italy). *J. Geophys. Res.* 101, 17467–17480.
- Bonaccorso, et al., 2004a. In: Bonaccorso, A., Calvari, S., Coltelli, M., Del Negro, C., Falsaperla, S. (Eds.), Mount Etna: Volcano Laboratory. *Am. Geophys. Union Geophys. Monogr.*, vol. 143.
- Bonaccorso, A., D'Amico, S., Mattia, M., Patanè, D., 2004b. Intrusive mechanisms at Mt. Etna forerunning the July–August 2001 eruption from seismic and ground deformation data. *Pure Appl. Geophys.* 161, 1469–1487.
- Branca, S., Carbone, D., Greco, F., 2003. Intrusive mechanism of the 2002 NE-Rift eruption at Mt. Etna (Italy) inferred through continuous microgravity data and volcanological evidences. *Geophys. Res. Lett.* 30, 2077.
- Carbone, D., Greco, F., 2007. Review of microgravity observations at Mt. Etna: a powerful tool to monitor and study active volcanoes. *Pure Appl. Geophys.* 164, 769–790.
- Castellano, M., Bianco, M.F., Imposi, S., Milano, G., Menza, S., Vilardo, G., 1997. Recent deep earthquake occurrence at Mt. Etna (Sicily, Italy). *Phys. Earth Planet. Inter.* 102, 277–289.
- Cayol, V., Cornet, F.H., 1998. Effects of topography on the interpretation of the deformation field of prominent volcanoes – application to Etna. *Geophys. Res. Lett.* 25, 1979–1982.
- Cheng, C.H., Johnston, D.H., 1981. Dynamic and static moduli. *Geophys. Res. Lett.* 8, 39–42.
- Ciccotti, M., Mulargia, F., 2004. Differences between static and dynamic elastic moduli of a typical seismogenic rock. *Geophys. J. Int.* 157, 474–477.
- Ciccotti, M., Negri, N., Sassi, L., Gonzato, G., Mulargia, F., 2000. Elastic and fracture parameters of Etna, Stromboli, and Vulcano lava rocks. *J. Volcanol. Geotherm. Res.* 98, 209–217.
- Ciccotti, M., Almagro, R., Mulargia, F., 2004. Static and dynamic moduli of the seismogenic layer in Italy. *Rock Mech. Rock Eng.* doi:10.1007/s00603-003-0019-7.
- Cox, S.J.D., Meredith, P.G., 1993. Microcrack formation and material softening in rock measured by monitoring acoustic emissions. *Int. J. Rock Mech. Min. Sci. Geomech. Abstr.* 30, 11–24.
- Eberhardt, E., Stead, D., Stimpson, B., 1999. Quantifying progressive pre-peak brittle fracture damage in rock during uniaxial compression. *Int. J. Rock Mech. Min. Sci.* 36, 361–380.
- Eissa, E.A., Kazi, A., 1989. Relation between static and dynamic Young's moduli of rocks. *I Int. J. Rock Mech. Min. Sci. Geomech. Abstr.* 25, 479–482.

- Fortin, J., Schubnel, A., Guéguen, Y., 2005. Elastic wave velocities and permeability evolution during compaction of Bleurswiller sandstone. *Int. J. Rock Mech. Min. Sci.* 42, 873–889.
- Glover, P.W.J., Baud, P., Darot, M., Meredith, P.G., Boon, S.A., LeRevelec, M., Zoussi, S., Reuschle, T., 1995. α/β phase transition in quartz monitored using acoustic emissions. *Geophys. J. Int.* 120, 775–782.
- Guéguen, Y., Schubnel, A., 2003. Elastic wave velocities and permeability of cracked rocks. *Tectonophysics* 370, 163–176.
- Guest, J.E., 1982. Styles of eruption and flow morphology on Mt. Etna. *Mem. Soc. Geol. Ital.* 23, 49–73.
- Hadley, K., 1976. Comparison of calculated and observed crack densities and seismic velocities in Westerly granite. *J. Geophys. Res.* 81, 3484–3494.
- Hawkes, I., Mellor, M., 1970. Uniaxial testing in rock mechanics laboratories. *Eng. Geol.* 4, 177–285.
- Heap, M.J., Faulkner, D.R., 2008. Quantifying the evolution of static elastic properties as crystalline rock approaches failure. *Int. J. Rock Mech. Min. Sci.* 45, 564–573.
- Hickman, S.H., Evans, B., 1987. Influence of geometry on crack healing rate in calcite. *Phys. Chem. Miner.* 15, 91–102.
- Hill, D.P., 1977. A model for earthquake swarms. *J. Geophys. Res.* 82, 1347–1352.
- Holcomb, D., 1993. General theory of the Kaiser effect. *Int. J. Rock Mech. Min. Sci. Geomech. Abstr.* 30, 929–935.
- Kaiser, L., 1953. Erkenntnisse und folgerungen aus der messung von geräuschen bei zugbeanspruchung von metallischen werkstoffen. *Arch. Eisenhüttenwesen* 24, 43–45.
- Kilburn, C.R.J., 2003. Multiscale fracturing as a key to forecasting volcanic eruptions. *J. Volcanol. Geotherm. Res.* 125, 271–289.
- Lau, J.S.O., Chandler, N.A., 2004. Innovative laboratory testing. *Int. J. Rock Mech. Min. Sci.* 41, 1427–1445.
- Lavrov, A., 2003. The Kaiser effect in rocks: principals and stress estimation techniques. *Int. J. Rock Mech. Min. Sci.* 40, 151–171.
- Lockner, D., 1993. The role of acoustic emission in the study of rock fracture. *Int. J. Rock Mech. Min. Sci. Geomech. Abstr.* 30, 883–899.
- Lombardo, G., Cardaci, C., 1994. The seismicity of the Etnean area and different features of observed seismic sequences. *Acta Vulcanol.* 5, 155–163.
- Martin, C.D., Chandler, N.A., 1994. The progressive fracture of Lac du Bonnet granite. *Int. J. Rock Mech. Min. Sci.* 31, 643–659.
- Mogi, K., 1966. Some precise measurements of fracture strength of rocks under uniform compressive stress. *Rock Mech. Eng. Geol.* 4, 41–55.
- O'Connell, R.J., Budiansky, B., 1974. Seismic velocities in dry and saturated cracked solids. *J. Geophys. Res.* 79, 5412–5426.
- Patanè, G., Montalto, A., Vinciguerra, S., Tanguy, J.C., 1996. A model of the 1991–1993 eruption onset of Etna (Italy). *Phys. Earth Planet. Inter.* 97, 231–245.
- Patanè, D., De Gori, P., Chiarabba, C., Bonaccorso, A., 2003. Magma ascent and the pressurization of Mount Etna's volcanic system. *Science* 299, 2061–2063.
- Patanè, D., Cocina, O., Falsaperla, S., Privitera, E., Spampinato, S., 2004. Mt. Etna volcano: a seismological framework. In: Bonaccorso, A., Calvari, S., Coltelli, M., Falsaperla, S. (Eds.), *Mt. Etna: Volcano Laboratory*. AGU Geophysical Monograph, vol. 143, pp. 147–166.
- Patanè, D., Barberi, G., Cocina, O., De Gori, P., Chiarabba, C., 2006. Time-resolved seismic tomography detects magma intrusions at Mount Etna. *Science* 313, 821–823.
- Reuschlé, T., Gbaguidi Haore, S., Darot, M., 2003. Microstructural control on the elastic properties of thermally cracked granite. *Tectonophysics* 370, 95–104.
- Rocchi, V., Sammonds, P.R., Kilburn, C.R.J., 2004. Fracturing of Etnean and Vesuvian rocks at high temperatures and low pressures. *J. Volcanol. Geotherm. Res.* 132, 137–157.
- Roman, D.C., Cashman, K.V., 2006. The origin of volcano-tectonic earthquake swarms. *Geology* 34, 457–460.
- Sayers, C.M., Kachanov, M., 1995. Microcrack induced elastic wave anisotropy in brittle rocks. *J. Geophys. Res.* 100, 4149–4156.
- Simmons, G., Brace, W.F., 1965. Comparison of static and dynamic measurements of compressibility of rocks. *J. Geophys. Res.* 70, 5649–5656.
- Soga, N., Mizutani, H., Spetzler, H., Martin, R.J.L., 1978. The effect of dilatancy on velocity anisotropy in Westerly granite. *J. Geophys. Res.* 83, 4451–4458.
- Stanchits, S., Vinciguerra, S., Dresen, G., 2006. Ultrasonic velocities, acoustic emission characteristics and crack damage of basalt and granite. *Pure Appl. Geophys.* 163, 974–993.
- Takemura, T., Oda, M., 2005. Changes in crack density and wave velocity in association with crack growth in triaxial tests of Inada granite. *J. Geophys. Res.* 110, B05401. doi:10.1029/2004JB003395.
- Tanguy, J.-C., Condomines, M., Kieffer, G., 1997. Evolution of the Mount Etna magma: Constraints on the present feeding system and eruptive mechanism. *J. Volcanol. Geotherm. Res.* 75, 221–250.
- Tibaldi, A., Groppelli, G., 2002. Volcano-tectonic activity along structures of the unstable NE flank of Mt. Etna (Italy) and their possible origin. *J. Volcanol. Geotherm. Res.* 115, 277–302.
- Ukawa, M., Tsukahara, H., 1996. Earthquake swarms and dike intrusions off the east coast of Izu Peninsula, central Japan. *Tectonophysics* 253, 285–303.
- Vinciguerra, S., Lator, V., Bocciato, S., Kamimura, R.T., 2001. Identifying and discriminating seismic patterns leading flank eruptions at Mt. Etna Volcano during 1981–1996. *J. Volcanol. Geotherm. Res.* 106, 211–228.
- Vinciguerra, S., Trovato, C., Meredith, P.G., Benson, P.M., 2005. Relating seismic velocities, thermal cracking and permeability in Mt. Etna and Iceland basalts. *Int. J. Rock Mech. Min. Sci.* 42, 900–910.
- Vinciguerra, S., Trovato, C., Meredith, P.G., Benson, P.M., Troise, C., De Natale, G., 2006. Understanding the seismic velocity structure of Campi Flegrei caldera (Italy): from the laboratory to the field scale. *Pure Appl. Geophys.* 163, 2205–2221.
- Walsh, J.B., 1965. The effect of cracks on the compressibility of rock. *J. Geophys. Res.* 70, 381–389.
- Winkler, K.W., Murphy III, W.F., 1995. Acoustic velocity and attenuation in porous rocks. In: Ahrens, T.J. (Ed.), *Rock Physics and Phase Relations*. AGU reference shelf, pp. 20–34.